THE JOURNAL OF BIOLOGICAL CHEMISTRY
Vol. 276, No. 26, Issue of June 29, pp. 24186–24193, 2001

*Printed in U.S.A.*

# Structure of a Pilin Monomer from *Pseudomonas aeruginosa*

## IMPLICATIONS FOR THE ASSEMBLY OF PILI*

Received for publication, January 24, 2001, and in revised form, March 13, 2001
Published, JBC Papers in Press, April 9, 2001, DOI 10.1074/jbc.M100659200

**David W. Keizer‡, Carolyn M. Slupsky‡, Michal Kalisiak‡§, A. Patricia Campbell¶, Matthew P. Crump‖, Parimi A. Sastry§, Bart Hazes§, Randall T. Irvin‡§, and Brian D. Sykes‡****

*From the ‡Protein Engineering Network Centres of Excellence (PENCE), 713 Heritage Medical Research Centre, University of Alberta, Edmonton, Alberta T6G 2S2, Canada, the §Department of Medical Microbiology and Immunology, University of Alberta, Edmonton, Alberta T6G 2H7, Canada, the ‖Department of Biochemistry, University of Southampton, Bassett Crescent East, Southampton SO16 7PX, United Kingdom, and the ¶Department of Medicinal Chemistry, School of Pharmacy, University of Washington, Seattle, Washington 98195*

**Type IV pilin monomers assemble to form fibers called pili that are required for a variety of bacterial functions. Pilin monomers oligomerize due to the interaction of part of their hydrophobic N-terminal α-helix. Engineering of a truncated pilin from *Pseudomonas aeruginosa* strain K122-4, where the first 28 residues are removed from the N terminus, yields a soluble, monomeric protein. This truncated pilin is shown to bind to its receptor and to decrease morbidity and mortality in mice upon administration 15 min before challenge with a heterologous strain of *Pseudomonas*. The structure of this truncated pilin reveals an α-helix at the N terminus that lies across a 4-stranded antiparallel β-sheet. A model for a pilus is proposed that takes into account both electrostatic and hydrophobic interactions of pilin subunits as well as previously published x-ray fiber diffraction data. Our model indicates that DNA or RNA cannot pass through the center of the pilus, however, the possibility exists for small organic molecules to pass through indicating a potential mechanism for signal transduction.**

*Pseudomonas aeruginosa* is a common, rod-shaped, Gram-negative bacterium that is an opportunistic pathogen and frequently causes life-threatening infections in burn, cancer, cystic fibrosis, immuno-compromised, and intensive care patients (1–3). The initial stage of *Pseudomonas* infection is the adherence of the pathogen to the mucosal cells of a susceptible host, which is mediated by a type IV pilus (2–5). These type IV pili are produced by a variety of bacterial pathogens, including *Pseudomonas*, *Neisseria, Moraxella, Dichelobacter,* and *Vibrio*. While type IV pili are critical virulence factors, they also play a central role in twitching motility (6), DNA transformation, and bacteriophage absorption (7). Type IV pili are long fibers that extend from the bacterial surface and are composed of a single structural protein, pilin. These pili are ~1,000–4,000 nm long, 5.2 nm in outer diameter (4, 8) and can be lengthened or retracted by assembly or disassembly of pilin subunits at the base of the pilus. The retraction of the pilus powers twitching motility and gliding motility (9).

Pilin is encoded by the *pil*A gene of the *pil* operon (10), and is initially synthesized as a precursor, pre-pilin, which is cleaved, *N*-methylated, and assembled into a pilus. Each pilin protein contains a functional receptor-binding site; however, binding sites are only displayed at the tip of the pilus (11). This region is proposed to be the point of first contact between bacterial and host cells; consequently, pilus-mediated binding is considered a tip-associated event (11). Up to five pilin monomers are exposed at the tip of the pilus, resulting in multivalent receptor binding as is common for lectin-carbohydrate interactions (12). The multivalency of the pilus and its variability in length have confounded the determination of accurate affinity constants for the pilus-cell surface interaction and prevented a comparison of the binding affinities of pili and synthetic receptor-binding domains.

The C-terminal receptor-binding domain of pilin has been studied in detail for many different strains of *P. aeruginosa*. Extensive structural analysis of free peptides that form the C-terminal-binding domain has shown the presence of a type I β-turn followed by a type II β-turn (13, 14). Interestingly, the *Neisseria gonorrhoeae* strain MS-11 pilin contains two type I β-turns rather than a type I turn followed by a type II turn that is seen in PAK[1] and PAO (13, 15, 16). The major host cell-surface receptors for the *P. aeruginosa* pilin C-terminal receptor-binding domains are the common cell surface glycosphingolipids asialo-GM1 and asialo-GM2 (5, 17–20) which are up-regulated in susceptible patients. The minimal portion of the cell surface receptors asialo-$G_{M1}$ and asialo-$G_{M2}$ recognized by the receptor-binding domain consists of the disaccharide βGalNAc(1–4)βGal (18–20).

*P. aeruginosa* has both high innate resistance and a high frequency of acquired anti-microbial resistance (21). Treatment of *P. aeruginosa* infections is frequently problematic and associated with high morbidity and mortality rates in susceptible

* This study was supported by the Canadian Bacterial Diseases Network, the Protein Engineering Network Centers of Excellence, the Canadian Institutes of Health Research, and Cytovax Biotechnologies Inc. The costs of publication of this article were defrayed in part by the payment of page charges. This article must therefore be hereby marked "*advertisement*" in accordance with 18 U.S.C. Section 1734 solely to indicate this fact.

*The atomic coordinates and structure factors (code 1HPW) have been deposited in the Protein Data Bank, Research Collaboratory for Structural Bioinformatics, Rutgers University, New Brunswick, NJ (http://www.rcsb.org/).*

** To whom correspondence should be addressed: PENCE,713 Heritage Medical Research Center, Edmonton, Alberta T6G 2S2, Canada. Fax: 780-492-1473; Tel.: 780-492-6540; E-mail: brian.sykes@ualberta.ca.

[1] The abbreviations used are: PAK, *Pseudomonas aeruginosa* strain K; DQF-COSY, double-quantum-filtered correlated spectroscopy; HSQC, heteronuclear single quantum coherence; LB, Luria broth; MS-11, *Neisseria gonorrhoeae* strain MS-11; NOESY, nuclear Overhauser enhancement spectroscopy; PAO, *P. aeruginosa* strain O; PBS, phosphate-buffered saline; r.m.s., root mean square; TOCSY, total correlation spectroscopy; βGalNAc(1–4)βGal, 2-acetamido-2-deoxy-β-D-galactopyranosyl-β-D-galactopyranoside; asialo-GMI, gangliotetraosyl ceramide; asialo-GM2, gangliotriaosyl ceramide.

patient groups. Thus there is a significant interest in developing a vaccine against *Pseudomonas*. Antibodies have been raised against several proteins expressed by the bacteria including elastase, exotoxin A, and lipoprotein I (22–24) as well as against various polysaccharides (25). The C-terminal receptor-binding domain of pilin has been a natural target for vaccine development due to its early role in the attachment and infection process. The feasibility of using type IV pilus vaccines has been effectively demonstrated in both sheep and cattle where protection against *Dichelobacter nodosus* and *Moraxella bovis,* respectively, has been observed with pili-based vaccines (26, 27). A free peptide of this domain from PAK has been successfully used to produce monoclonal and polyclonal antibodies that confer protection in an animal infection model (28). Synthetic peptide analogues based on this domain have been used to produce antibodies that show cross-reactivity between different *P. aeruginosa* strains (29) and have been successfully used to generate vaccines.

Herein, we describe the structure of a truncated, monomeric type IV pilin from *P. aeruginosa* strain K122-4 using NMR spectroscopy. The first 28 residues were truncated to prevent oligomerization. We demonstrate that this truncated protein retains the biological characteristics of the intact pilin monomer. This monomeric pilin is able to compete for receptor binding sites with a heterologous strain of *Pseudomonas* resulting in a significant decrease in mortality in an animal infection model. It follows, therefore, that the pilin monomer also retains the biological characteristics of the pilus fiber except for the oligomerization properties of the N-terminal 28 residues. We have developed a model for the formation of the pilus fiber based on electrostatic interactions between the globular portion of the pilin protein and previous x-ray diffraction data on pilus fibers (8). Currently, this model is the best fit to the x-ray fiber diffraction data. The results presented here contribute significantly to our understanding of the structure and function of type IV pili and will aid in the development of novel therapeutic strategies for managing and preventing *Pseudomonas* infections.

## EXPERIMENTAL PROCEDURES

*Protein Samples*—A DNA sequence encoding *P. aeruginosa* strain K122-4 pilin$^{(29-150)}$ was polymerase chain reaction-amplified from the full-length K122-4 pilin cDNA and cloned into the pRLD expression vector such that it had an in-frame OmpA leader sequence fused to the truncated pilin (30) using standard techniques. Unlabeled and $^{15}$N labeled K122-4 pilin$^{(29-150)}$ was prepared from *Escherichia coli* DH5$\alpha$ cells, transformed with the pRLD plasmid carrying the K122-4 pilin$^{(29-150)}$ gene, grown in LB or minimal media containing $^{15}NH_4Cl$. K122-4 pilin$^{(29-150)}$ was extracted from the periplasm by osmotic shock and purified by cation exchange with a CM-cellulose column (utilizing a linear gradient of 0–0.8 M NaCl) in 10 mM sodium acetate, pH 4.5. K122-4 pilin$^{(29-150)}$ was subsequently desalted on a Sephadex G75 column and lyophilized. The protein was deemed >95% pure by reverse phase high performance liquid chromatography analysis. The molecular weight of the sample was confirmed by electrospray mass spectroscopy using a Fisons VG Quattro mass spectrometer. The identity of the purified product was confirmed by N-terminal amino acid sequencing and immunoblotting using rabbit polyclonal anti-K122-4 pilus antisera. NMR analysis was performed on ~0.5 mM K122-4 pilin$^{(29-150)}$ dissolved in either 90% $H_2O$, 10% $D_2O$ or 99% $D_2O$ containing 20 mM deuterated sodium acetate, 1 mM $NaN_3$, and 1 mM 2,2-dimethyl-2-silapentane-5-sulfonic acid, pH 5.0.

*Protein Characterization*—Sedimentation equilibrium analysis of K122-4 pilin$^{(29-150)}$ was performed with a Beckman XL-I analytical centrifuge with an AN50TI rotor at 20 °C. Data were collected using interference optics. Three protein concentrations were used: 0.75 mg ml$^{-1}$, 2.03 mg ml$^{-1}$ and 3.45 mg ml$^{-1}$, each in 20 mM sodium phosphate, pH 7.2, 100 mM sodium chloride. The molecular mass of the truncated pilin was calculated from the protein concentration gradient at sedimentation equilibrium using a partial specific volume of 0.7255 ml g$^{-1}$ as determined from the amino acid composition. Sedimentation equilibrium data was evaluated using a least-squares curve-fitting algorithm contained in the NonLin analysis program (31).

TABLE I
*Experimental restraints and structural statistics*

| | |
|---|---|
| Number of Experimental restraints | |
| Distance restraints from NOEs | 1032 |
| Intra ($i = j$) | 335 |
| Sequential ($\|i - j\| = 1$) | 357 |
| Short ($2 \leq \|i - j\| \leq 5$) | 120 |
| Long ($\|i - j\| \geq 6$) | 220 |
| Hydrogen bond restraints | 30 |
| Dihedral angle restraints | 181 |
| Phi | 68 |
| Psi | 86 |
| Chi-1 | 27 |
| Total experimental restraints | 1213 |
| R.m.s. deviations from experimental data | |
| NOEs | 0.0166± 0.002 Å |
| Dihedrals | 0.39± 0.11 degree |
| R.m.s. deviations from ideal stereochemistry | |
| Bonds | 0.00269± 0.00012 Å |
| Angles | 0.518± 0.011 degree |
| Ramachandran analysis | |
| Residues in favored regions | 66% |
| Residues in additional allowed regions | 28% |
| Residues in generously allowed regions | 5% |
| Residues in disallowed regions | 1% |

*NMR Spectroscopy*—NMR experiments were performed on Varian Unity 600 and INOVA 800 MHz spectrometers at 30 °C. Spectra were processed with NMRPipe (32) and analyzed using NMRView (33). $^1$H and $^{15}$N chemical shift assignments and may be found with BMRB accession number 4918 (34).

An ensemble of 25 K122-4 pilin$^{(29-150)}$ structures was generated from 1032 distance restraints, 30 hydrogen-bond and 181 dihedral angle restraints (PDB code 1HPW) by using the dynamic simulated annealing protocols of Nilges *et al*. (35) in the program X-PLOR version 3.8 (36). Interproton distance restraints were derived from a three-dimensional $^{15}$N-NOESY HSQC spectrum in $H_2O$ and a two-dimensional homonuclear NOESY spectra in $D_2O$ both with a $\tau_{mix}$ of 60 ms. NOEs were classified as strong, medium, or weak depending on their intensity. A list of NOE restraints used in structure calculations has been submitted to the PDB (code 1HPW). H-bonds were determined by observing a two-dimensional TOCSY spectrum collected 6 days after dissolving the protein sample in $D_2O$ buffer. 30 spin systems originating from backbone amide protons were observed and assigned as H-bonds after initial examination of ensembles of structures generated without incorporation of hydrogen bonds. $\phi$ Dihedral restraints were based on $^3J_{HNH\alpha}$ coupling constants measured in a high resolution HNHA spectrum (37). $\psi$ angles were determined by analysis of $d_{N\alpha}/d_{\alpha N}$ ratios but only incorporated into the regions of well defined secondary structure (38). Stereospecific assignments and $\chi^1$ restraints were obtained from the analysis of the $^3J_{\alpha\beta}$ coupling constants in DQF-COSY spectrum and the relative intensities of the NOEs from the NH and the $C_\alpha$ to $C_\beta$ protons in a 50-ms two-dimensional NOESY spectrum collected in $D_2O$. All structure calculations included the disulfide bonds, Cys$^{31}$-Cys$^{67}$ and Cys$^{103}$-Cys$^{116}$ restrained to a distance of 2.02 ± 0.1 Å. No distance violations greater than 0.2 Å nor dihedral violations greater than 2° were found. All nonglycine residues in disallowed ($\phi$, $\psi$) regions are located in the disordered termini of K122-4 pilin$^{(29-150)}$ (Table I).

*Receptor Binding Studies*—Pili from PAK were purified and biotinylated as described previously (20, 39). A polystyrene microtiter plate was coated with 50 $\mu$l of 40 $\mu$g ml$^{-1}$ asialo-GM$_1$ in methanol. The solvent was evaporated at room temperature. Nonspecific binding sites were blocked by the addition of 200 $\mu$l per well of 5% (w/v) bovine serum albumin, in PBS buffer (150 mM NaCl, 10 mM sodium phosphate, pH 7.2). The plate was incubated at 37 °C for 1.5 h and the wells were then washed 3 times with 250 $\mu$l of 0.05% (w/v) bovine serum albumin in PBS buffer. 50-$\mu$l aliquots of biotinylated PAK pili (0.88 $\mu$g ml$^{-1}$ in PBS buffer) containing various concentrations of the K122-4 pilin$^{(29-150)}$ were added to each well. The plate was incubated 2 h at 37 °C, washed (5 times with 250 $\mu$l of PBS buffer), followed by the addition of 50 $\mu$l/well of streptavidin-alkaline phosphatase conjugate at a 1:3000 dilution in PBS. The plate was then incubated for 1 h at room temperature, washed 5 times with 250 $\mu$l of PBS buffer, followed by the addition of 80 $\mu$l/well of the substrate solution (1 mg ml$^{-1}$ *p*-nitrophenyl phosphate in 10% (v/v) diethanolamine, pH 9.8). Following a 10-min incu-

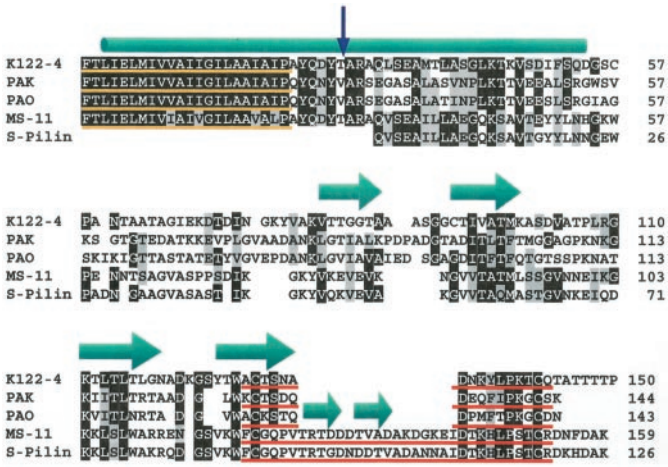


FIG. 1. **Alignment of the sequences of pilin proteins from *P. aeruginosa* strains K122-4, PAK, and PAO and *N. gonorrhoeae* strain MS-11.** In addition, an S-pilin from *N. gonorrhoeae* strain FA1090 was included in the alignment. The positions of highly conserved amino acids are highlighted in *black* (three or more members identical), and those of moderately conserved residues in *gray*. The depiction of secondary structural elements are based on an average of the start and stop points for each structural element over the first four solved structures. The N-terminal $\alpha$-helix is illustrated as a cylinder and the four $\beta$-strands are illustrated as *arrows*. Two additional $\beta$-strands are found near the C terminus of the sequences from *N. gonorrhoeae*. The oligomerization domains (residues 1–22) are *underlined* in *yellow*, and the C-terminal receptor-binding domain is *underlined* in *red*. A blue arrow depicts where K122-4 pilin was truncated for this study. The alignment was produced using the X-ALIGN software (64).

bation at room temperature, microtiter plates were read at 405 nm.

*Mice Infection Study*—This study was performed in accordance with the Canadian Animal Care Guidelines and with the ethical approval of the University of Alberta Health Science Animal Welfare Committee. The A.BY/SnJ mice used in the study are a strain developed by Jackson Laboratory (Bar Harbor, ME) that are highly susceptible to *Pseudomonas* infection (40), with the $LD_{50}$ for PAK being $\sim 3 \times 10^5$ colony forming units per mouse when challenged intraperitoneally (27). A.BY/SnJ mice were obtained from a breeding colony maintained behind barrier isolation. Mice were transferred from the breeding colony at 3 weeks of age and maintained in filtertop cages with a diet consisting of Purina PMI Certified Rodent Diet 5002 until they were ~10 weeks of age and had a weight of 18–20 g. A double-blind study was then established where groups of 10 mice were administered, intraperitoneally, 100 $\mu$l of PBS, pH 7.2, containing either bovine serum albumin (400 $\mu$g) or K122-4 pilin$^{(29-150)}$ (100, 200, or 400 $\mu$g). Fifteen minutes later, mice were challenged with ~5 times the $LD_{50}$ of PAK in 100 $\mu$l of LB administered intraperitoneally as previously described (27, 28). Mice were monitored hourly from 16 to 48 h post-challenge and euthanized when they displayed ruffled fur, evidence of dehydration, and had become non-responsive to stimuli.

## RESULTS

*Truncation of K122-4 Pilin*—K122-4 pilin has significant homology to the pilin sequences from other bacterial species (Fig. 1). The first 22 residues of pilin are highly conserved. These residues are highly apolar and extend from the rest of the protein. Consequently, they form an oligomerization domain in pilin. Pilin from *P. aeruginosa* strain K122-4 was engineered to exclude this oligomerization domain. The first 28 residues of the K122-4 pilin protein were therefore truncated to produce a protein that will be referred to herein as K122-4 pilin$^{(29-150)}$.

*Characterization of K122-4 Pilin$^{(29-150)}$*—The K122-4 pilin$^{(29-150)}$ was engineered to be exported to the periplasm by means of an OmpA leader sequence (30). This protein was subsequently processed such that a soluble monomeric K122-4 pilin$^{(29-150)}$ with an additional 7 residues (Ala-Leu-Glu-Gly-Thr-Glu-Phe numbered 22–28 in this article), were fused to the

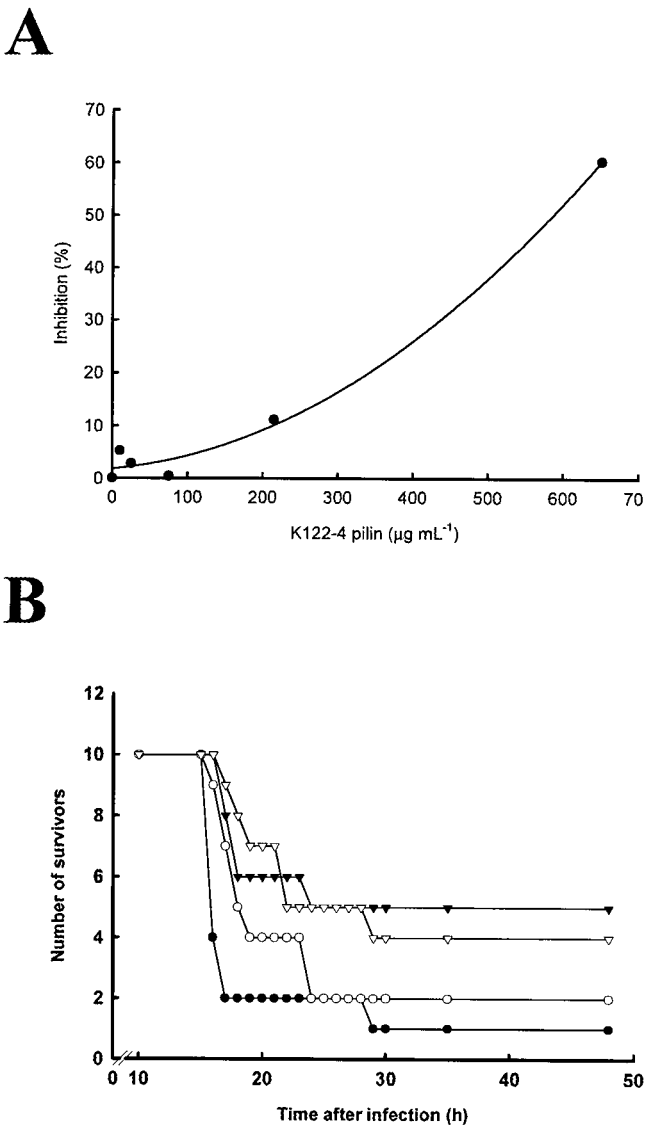


FIG. 2. *A,* K122-4 pilin$^{(29-150)}$ competitively inhibits the binding of biotinylated PAK pili to the asialo-$G_{M1}$ receptor. Inhibition is expressed as a percentage of the decrease in the amount of biotinylated PAK pili bound to the asialo-$G_{M1}$ receptor as a function of the concentration of K122-4 pilin$^{(29-150)}$. *B,* influence, in a murine infection model, of pretreatment with K122-4 pilin$^{(29-150)}$ on the outcome of a challenge with PAK. Pilin was administered intraperitoneally to A.BY/SnJ mice at 100 (○), 200 (▽), and 400 $\mu$g (▼) per mouse. Bovine serum albumin (●) was used as a control at 400 $\mu$g/mouse. Mice were challenged IP with wild type PAK at a dose of $1.6 \times 10^6$ colony forming units/mouse, 15 min after receiving K122-4 pilin$^{(29-150)}$.

N terminus of the K122-4 pilin$^{(29-150)}$ native sequence. The purified protein was subsequently analyzed by mass spectroscopy, analytical ultracentrifugation, and NMR. The mass of the purified protein was observed to be 13,107 Da by electrospray mass spectroscopy. Sedimentation equilibrium studies indicated a single homogeneous species with a molecular mass of 13,077 Da. Both of these values were in good agreement with the calculated molecular mass of the monomer (13,105 Da). A rotational correlation time of 7.4 ns was determined by NMR spectroscopic methods, which corresponds to a species of ~14 kDa at 30 °C (41). Taken together, these data indicate that K122-4 pilin$^{(29-150)}$ is monomeric up to the 0.5 mM concentrations used for NMR.

*K122-4 Pilin$^{(29-150)}$ Retains the Functional Characteristics of the Full-length Pilin Protein*—To determine if the truncated form of the pilin protein from K122-4 was correctly folded and

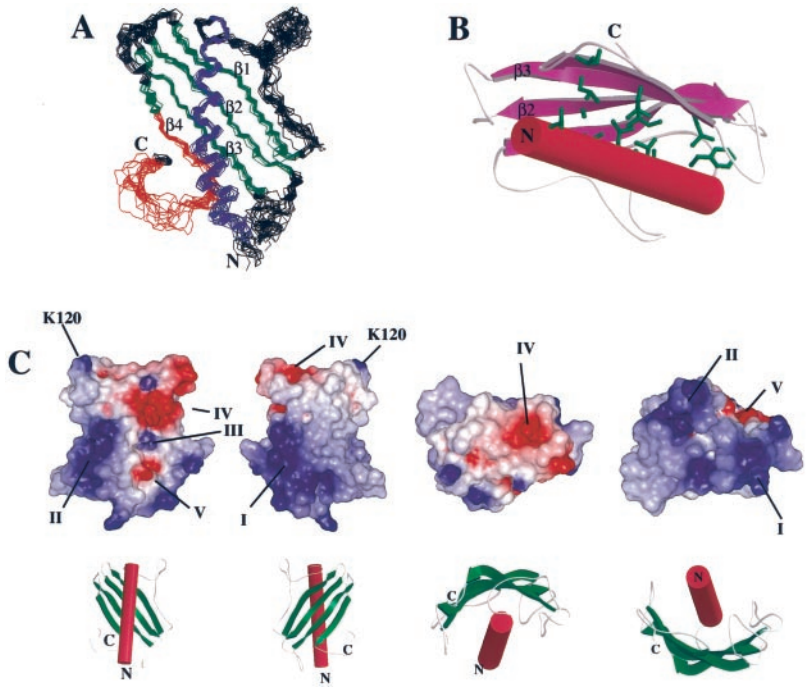


FIG. 3. **The tertiary structure of K122-4 pilin$^{(29-150)}$ was determined by NMR methods.** *A,* superimposition of the main chain atoms from the 10 lowest energy NMR-derived structures of K122-4 pilin$^{(29-150)}$ (PDB code 1HPW) superimposed using residues 31–54, 78–87, 91–100, 110–119, and 124–133. The $\alpha$-helix is colored in *blue*, the $\beta$-sheets are colored in *green,* and the C-terminal receptor binding domain (which includes part of the last $\beta$-sheet) is colored in *red*. The disordered N and C termini (residues 22–28 and 143–150) have been omitted for clarity. *B,* the hydrophobic residues interacting at the interface between the $\alpha$-helix and $\beta$-sheets serve to sandwich the $\alpha$-helix at approximately a 45° angle across the $\beta$-sheets. *C,* electrostatic surfaces generated using Delphi in InsightII illustrating the differential charge distribution on the surface of K122-4 pilin$^{(29-150)}$. The orientation of each surface is shown *below* in Molscript format. *Red* represents a negatively charged surface whereas *blue* represents a positively charged surface. The labeling of charged clusters is described in the text. The figure was prepared using InsightII and Molscript.

functional, two separate experiments were performed: binding of the truncated pilin to asialo-$G_{M1}$, which requires a functional receptor-binding domain (the C-terminal loop), and protection of mice from *P. aeruginosa* infection by injection with the truncated K122-4 pilin$^{(29-150)}$.

To determine if K122-4 pilin$^{(29-150)}$ retains receptor-binding function, a competitive inhibition assay was performed. The assay involved competitive binding between K122-4 pilin$^{(29-150)}$ and PAK pili (composed of the full-length PAK pilin protein assembled into pili) with the pili receptor, the naturally occurring membrane glycosphingolipid, asialo-$G_{M1}$. PAK pili were chosen for the assay as they bind to the same receptors as K122-4 pili, are the best characterized and most readily purified pilus type, and are the most extensively studied pili from *P. aeruginosa*. The truncated K122-4 pilin$^{(29-150)}$ competitively inhibits PAK pili binding to immobilized asialo-$G_{M1}$ in a dose-dependent manner (Fig. 2*A*). This suggests that the K122-4 pilin$^{(29-150)}$ monomer retains receptor-binding capability, and that the receptor-binding domain is intact in the truncated protein.

To determine if K122-4 pilin$^{(29-150)}$ could protect mice against *Pseudomonas* infection, a double-blind study using A.BY/SnJ mice was carried out. Intraperitoneal administration of purified K122-4 pilin$^{(29-150)}$ in mice was found to delay and decrease mortality by infection with PAK (Fig. 2*B*). The protection afforded by K122-4 pilin$^{(29-150)}$ appears to be dose-dependent, with both the 200 and 400 $\mu$g of dose of K122-4 pilin$^{(29-150)}$ conferring substantial protection against infection for over 35 h.

*Description and Quality of the Structure of K122-4 Pilin$^{(29-150)}$*—The structure of K122-4 pilin$^{(29-150)}$ was determined using NMR spectroscopy (Fig. 3). The C-terminal portion of the protein folds into a four-stranded antiparallel $\beta$-sheet structure composed of residues 78–87, 91–100, 110–119, and 126–133. This $\beta$-sheet structure folds around an $\alpha$-helix that is comprised of residues near the N terminus (31–54). The $\alpha$-helix lies at approximately a 45° angle from the axis of the $\beta$-sheet (Fig. 3*B*). Most of the hydrophobic residues point into the center of the molecule anchoring the helix across the $\beta$-sheet. The outer surface of the molecule is composed primarily of polar residues. The hydrophobic interface between the helix and the four $\beta$-strands, as well as the loops between them, is comprised of residues Leu$^{33}$, Leu$^{39}$, Leu$^{43}$, Val$^{47}$, Ile$^{50}$, and Phe$^{51}$ of the $\alpha$-helix with residues Val$^{81}$, Ala$^{87}$, Ile$^{95}$, Ala$^{97}$, Leu$^{113}$, Leu$^{115}$, Leu$^{117}$, Trp$^{127}$, and Leu$^{138}$. These residues, for the most part, appear to be conserved (Fig. 1). The secondary structural elements constitute a well defined bundle with r.m.s. distributions about the mean coordinate positions of 0.71 ± 0.18 Å for backbone atoms, and 1.08 ± 0.17 Å for all heavy atoms. The loop structures (residues 28–30, 55–77, 88–90, 101–109, 120–125, and 134–150) connecting the $\alpha$-helix and $\beta$-strands are not as well defined. Except for residues 76 and 77, these residues tend to display random coil amide 1HN and $^{15}$N chemical shifts and high r.m.s. deviations within the ensemble of calculated structures. The first 7 residues of K122-4 pilin$^{(29-150)}$, that precede the actual protein sequence starting at residue 29, are completely disordered and thus will not be discussed further.

The C-terminal receptor-binding domain of K122-4 pilin is composed of residues Ala$^{128}$-Gln$^{143}$. As with peptide studies of this region (14, 42), a $\beta$-turn was found involving residues Asp$^{134}$, Asn$^{135}$, Lys$^{136}$, and Tyr$^{137}$. A second $\beta$-turn involving residues Pro$^{139}$, Lys$^{140}$, Thr$^{141}$, and Cys$^{142}$ could not be unambiguously determined, due mainly to the fact that resonances from residues Pro$^{139}$, Lys$^{140}$, and Thr$^{141}$ could not be assigned due to NMR spectral overlap, resulting in poor definition of this region in the K122-4 pilin$^{(29-150)}$ structure. We expect that this portion of the receptor-binding domain does indeed form another $\beta$-turn by homology to the peptide studies and the crystal structures of PAK and *N. gonorrhoeae* strain MS-11. The first 5 residues of the receptor-binding domain of K122-4 pilin$^{(29-150)}$ is composed of residues in the last strand of the $\beta$-sheet resulting in a highly defined structured region that is not observed in isolated peptides from this C-terminal region (42, 43).

The K122-4 pilin$^{(29-150)}$ protein has an unusual charge distribution, as the charges are not distributed evenly on the surface of the molecule, but tend to be clustered in 5 regions (Fig. 3*C*). Basic residues are clustered in three regions: (i) Lys$^{76}$, Lys$^{80}$, Lys$^{100}$, Lys$^{109}$, and Lys$^{111}$ (on the side of the pilus that faces the solvent), (ii) Arg$^{30}$, Lys$^{44}$, Lys$^{136}$, and Lys$^{140}$ (near the C-terminal binding loop), and (iii) Lys$^{69}$ and Lys$^{46}$ (on

the C-terminal side of the helix near the acidic cluster). The acidic residues are clustered in two major regions: (iv) $Asp^{49}$, $Asp^{54}$, $Glu^{68}$, $Asp^{70}$, and $Asp^{72}$ (along with $Gln^{53}$, $Asn^{60}$, and $Asn^{74}$) located C-terminal to the helix and (v) $Glu^{35}$, $Asp^{103}$, and $Asp^{134}$ (along with $Gln^{32}$, $Asn^{131}$, $Asn^{135}$, and $Gln^{143}$) located on the N-terminal side of the helix. Thus distinct positive and negative regions exist on the molecule.

## DISCUSSION

The C-terminal 122 residues of the type IV pilin from K122-4 adopt a distinctive fold whereby the N-terminal $\alpha$-helix is surrounded by a set of four curved antiparallel $\beta$-strands. This fold closely resembles the x-ray crystal structures of pilin from *N. gonorrhoeae* strain MS-11 (PDB code 1AY2, Ref. 14) and a similarly truncated version from PAK (PDB code 1DZ0, Ref. 15) (Fig. 4). 40% Pairwise amino acid identity exists between pilin sequences of *P. aeruginosa* strain K122-4 and PAK. Despite the large evolutionary differences between the genera *Neisseria* and *Pseudomonas*, 39% pairwise amino acid identity exists between the *N. gonorrhoeae* strain MS-11 pilin and the *P. aeruginosa* strain K122-4 pilin (Fig. 1). All three structures have a similar fold with a similar curvature of the $\beta$-sheet that surrounds the C-terminal portion of the $\alpha$-helix. The $\alpha$-helix of K122-4 pilin$^{(29-150)}$ lies at approximately a 45° angle across the surface of the $\beta$-sheet, whereas in the PAK and *N. gonorrhoeae* strain MS-11 pilin crystal structures, the $\alpha$-helix is close to parallel to the $\beta$-sheet. This difference in structures is likely to be the result of an additional disulfide bond found in K122-4 pilin as well as the distribution of hydrophobic amino acids across the $\beta$-strands, which force the K122-4 pilin helix to lie at 45° (Fig. 3*B*). In addition, the structures of the C-terminal receptor-binding domains of all three proteins are similar. The major difference between the K122-4 pilin$^{(29-150)}$ structure and the *N. gonorrhoeae* strain MS-11 pilin structure is that the MS-11 pilin structure contains two $\beta$-strands that are not seen in the K122-4 pilin$^{(29-150)}$ sequence or structure (Figs. 1 and 4).

*Truncation of the Oligomerization Domain of the K122-4 Pilin Protein Does Not Affect the Structure*—Analysis of the sequence and structure of *N. gonorrhoeae* strain MS-11 pilin suggests that the first 30 residues form an extended helix that does not interact with the globular domain of the pilin. By homology, it follows that the first 28 residues of K122-4 pilin could be removed without affecting the fold of the remaining 122 residues. Truncation of part of the N-terminal helix is not unprecedented, as there are naturally occurring type IV pilins, termed S-pilins, which are missing several residues at the N terminus (Fig. 1). *N. gonorrhoeae* S-pilin, produced by N-terminal cleavage after residue 39 (Fig. 1), is a stable soluble protein that is secreted into the extracellular environment (44, 45). Similar soluble type IV pilins have been described in *Moraxella*, where truncated pilins appear to be generated by a site-specific recombinase (46, 47) rather than proteolysis. S-pilins have been observed in *N. gonorrhoeae* infections in humans (48), but their role in pathogenesis remains unclear. It has been speculated that they could reduce antibody-mediated inactivation of pili by capturing pilus-specific antibodies (49).

It has not been previously established if N-terminal truncated forms of pilin retain their adhesion properties. Although there does not appear to be a naturally occurring truncated version of a *P. aeruginosa* pilin, K122-4 pilin$^{(29-150)}$ is nevertheless a good model for this class of pilins. Biophysical studies demonstrate that K122-4 pilin$^{(29-150)}$ is a monomer. Furthermore, K122-4 pilin$^{(29-150)}$ retains its receptor binding capability as shown in a competitive inhibition assay with PAK pili using the natural receptor asialo-$G_{M1}$ (Fig. 2*A*). In addition, administration of K122-4 pilin$^{(29-150)}$ was able to confer some protection from subsequent challenge with a heterologous strain of *P. aeruginosa* in a mouse infection model (Fig. 2*B*). Presumably, K122-4 pilin$^{(29-150)}$ inhibits pili-mediated binding of the challenge organism within the peritoneal cavity by a competitive mechanism and inhibits the normal pathogenic mechanism of the infecting organism such that mortality rates in the infection model are reduced in a dose-dependent manner. There are several potential explanations for this behavior. (i) If the adhesion pilus plays a role in the dissemination of the pathogen from the initial infection site, blockage of the receptor could limit dissemination of the pathogen and thus reduce overall mortality. (ii) Alternatively, protection may ensue due to modulation of the murine inflammatory response by the truncated pilin. Several studies have suggested that pilus-receptor interactions result in elevated expression of interleukin-8. (iii) The initiation of host cell signaling by pili may be due to the oligomerization of cell-surface receptors through multivalent binding by the multiple receptor-binding domains displayed at the tip of the pilus. Thus, the monomeric nature of K122-4 pilin$^{(29-150)}$ could inhibit the oligomerization of those receptors, reducing the host inflammatory response and potentially decreasing the severity of an infection. These data provide additional evidence that monomeric K122-4 pilin$^{(29-150)}$

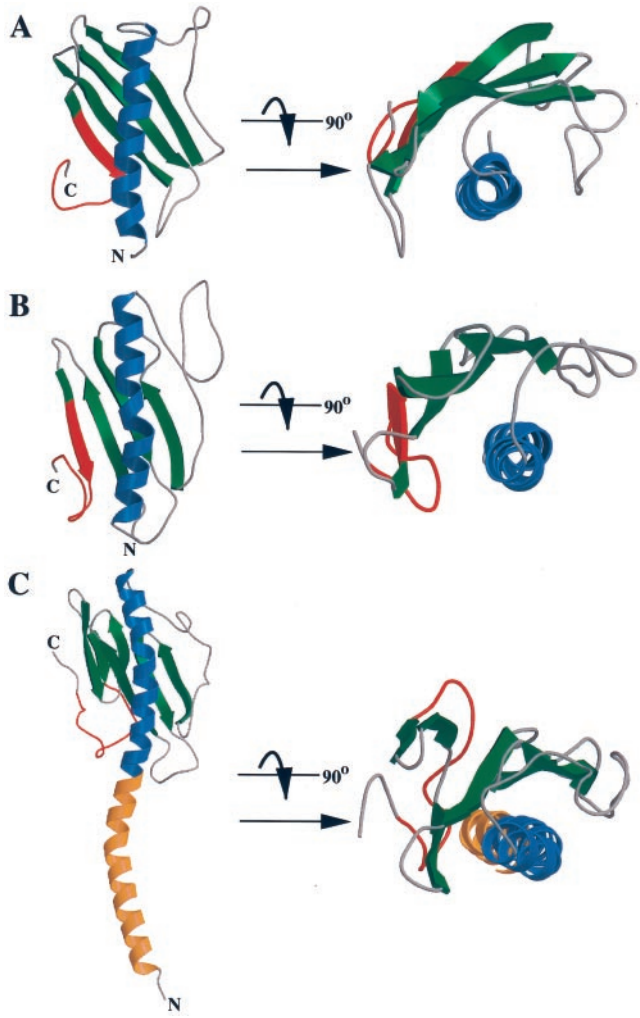


FIG. 4. **Molscript representations of the structures of pilin monomers from *P. aeruginosa* strains K122-4 and PAK as well as *N. gonorrhoeae* strain MS-11 showing the structural similarities.** *A,* K122-4 pilin$^{(29-150)}$. *B,* PAK pilin$^{(29-144)}$. *C,* full-length MS-11 pilin. The N-terminal $\alpha$-helix is shown in *blue*, the $\beta$-sheets are shown in *green*, the C-terminal receptor binding domain is shown in *red*, and the loop regions are shown in *gray*. The part of the N-terminal $\alpha$-helix in the MS-11 pilin that has been truncated from K122–4 and PAK is shown in *orange*. This figure was generated using Molscript.

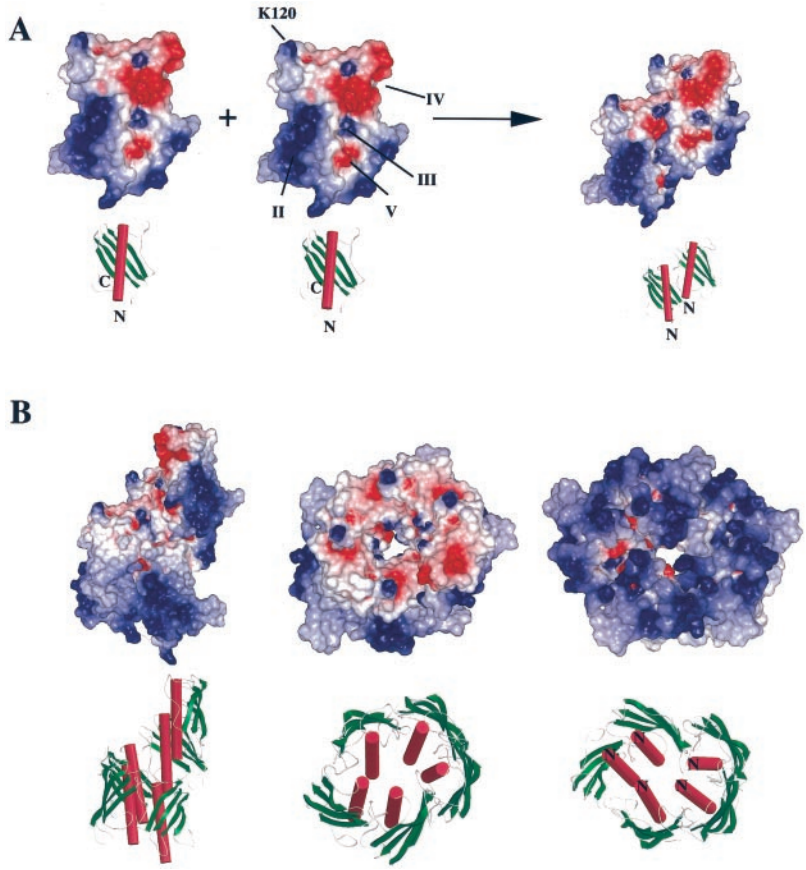


FIG. 5. **A proposed model for the formation of an intact pilus.** *A,* electrostatic complementarity allows the globular domains of K122-4 pilin$^{(29-150)}$ to interact slightly out of register. *B,* based on x-ray diffraction data (8), five K122-4 pilin monomers can associate to form one turn of a helical pilus structure. Using these data, a model was prepared by eye using electrostatic complementarity. For each turn of the pilus, complementary charged surfaces interact such that the positively charged surface present on the face at the N terminus of the truncated $\alpha$-helix interacts with the negatively charged surface present on the face at the C terminus of the $\alpha$-helix. The three views are a side view, a "top" view and a "bottom" view. The orientation of each surface is represented by a Molscript diagram. The charged surfaces were generated using Delphi in InsightII.

has retained a biologically relevant conformation. Therefore, in general, in addition to being possible antigenic decoys, S-pilins could reduce bacterial adherence by competing with cell-associated pili for receptors. Furthermore, S-pilins could also play a role in modulating the host response to infection by modulating pilus-induced cell signaling, as the protective effect observed with K122-4 pilin$^{(29-150)}$ could well be due to prevention of pilus-induced cell signaling and the subsequent modulation of the host inflammatory response.

Recently, there has been intense focus on the C-terminal receptor-binding domain of the pilin protein. This region consists of 17 residues from 128 to 145 (Fig. 1), and has been shown to bind asialo-$G_{M1}$, asialo-$G_{M2}$, and disaccharides such as $\beta$GalNAc(1–4)$\beta$Gal (20). In addition, the C-terminal receptor-binding domain is able to bind antibodies and hence is crucial for successful infection by *P. aeruginosa*. NMR studies of the C-terminal receptor-binding domain peptides of pilin from *P. aeruginosa* strains, PAK, PAO, and KB7 show evidence of a type I and a type II $\beta$-turn (42). *N. gonorrhoeae* strain MS11 pilin, however, was found to have two type I $\beta$-turns (15). In K122-4 pilin$^{(29-150)}$, one type I $\beta$-turn was found, however, the other turn region was less well defined due to a lack of NOE information because of spectral overlap. The fact that K122-4 pilin$^{(29-150)}$ can compete for receptor binding with intact PAK, suggests that the second $\beta$-turn is present.

*Assembly of Pilin Monomers into a Pilus Fiber*—A number of bacteria use type IV pili as adhesin molecules. However, the structural organization, morphogenesis, and dynamics of type IV pili are not completely understood (10). *In vitro*, the type IV pilus is remarkably stable and its dissociation requires the use of detergents (50). Nevertheless, *in situ*, the organism can readily lengthen or retract the pilus by either adding to or removing pilin monomers from the pilus filament in an energy dependent process (50, 51). Pilus retraction and twitching motility are significant virulence factors in animal infection models. This lengthening and retraction is believed to occur through highly regulated processes involving specific chaperones and pilus morphogenesis machinery. Despite the complex assembly apparatus, it has been observed that heterologous, and highly divergent pilins, can be expressed and properly assembled into pili in *P. aeruginosa* (52). Comparisons of type IV pilins show that the hydrophobic N-terminal 22 residues form the only region with a highly conserved amino acid sequence (Fig. 1). Furthermore, a glutamate to lysine mutation at position 5 of PAK pilin prevents pilus formation unless coexpressed with wild type pilin, in which case pili with altered morphology are formed (53). All these observations point to the fact that the N terminus is critical for pilus assembly.

*Model for the Pilus Fiber*—The structure presented here provides important additional clues for pilin assembly into a pilus fiber. A model for the association of pilin monomers into a pilus fiber was based on the structural studies presented here as well as previous x-ray fiber diffraction data on pilin fibers (8). The key features of this model are: (i) electrostatic surfaces of different monomers interact in a complementary manner (Fig. 5*A*). (ii) The monomers are offset such that they wind around in a helical manner with a left-handed twist (Fig. 5*B*). (iii) Approximately 5 subunits associate to form one turn of the helix. (iv) Hydrophobic N-terminal helices associate to form 5-helix bundles with $Glu^5$ interacting with the basic surface on the inside of the pilus globular portion (Fig. 6*E*) (possibly the conserved residue $Arg^{30}$). (v) The outer diameter of the pilus is ~52 Å with an inner diameter of the globular domains of 12 Å and a helical pitch of 41 Å (Fig. 6, *A* and *B*).

The impetus for generating the pilus model was the observation of electrostatic complementarity (Figs. 5 and 6, *C* and *D*). Distinct areas of positive and negative charges exist on the molecule allowing one to envisage a "lock and key" mechanism

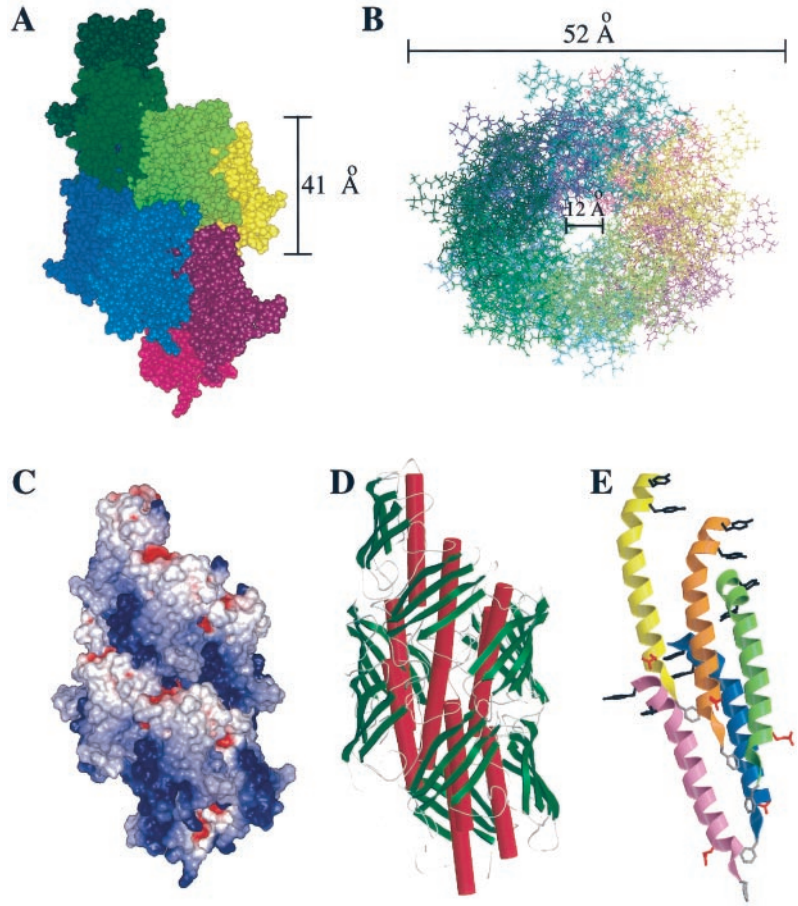


FIG. 6. **Model of two turns of a pilus structure.** *A,* a view of the van der Waals surface of part of a pilus. Each subunit (10 in total) is represented by a different color (one turn has *green* hues and the other turn has *blue* hues). The helical pitch of the pilus is ~41 Å, which is approximately the length of the globular domain when measured with the helix in a vertical position. *B,* a top view of a stick diagram of the pilus showing the diameter of the pilus to be ~52 Å with an "inner diameter" between the globular surfaces of ~12 Å. *C,* the Delphi electrostatic representation of two turns of the pilus. Note the banding pattern of a positively charged surface on the outside of the pilus. *D,* a Molscript representation of *C* showing that the helices are present on the interior of the pilus with the positive nature of the β-sheets on the exterior of the pilus. *E,* a proposed model of the oligomerization domain (residues 1–28) of K122-4 pilin. The α-helical structures were taken from the *N. gonorrhoeae* MS-11 crystal structure. The helices were oriented such that Phe 1 (*gray stick*) points toward the center of the helices, $Glu^{5}$ (*red stick*) points outward from the helices, Tyr-(*black stick*) points to the interface between the helices and $Tyr^{27}$ (*black stick*) points outward. Due to the extreme hydrophobic nature of this part of the N-terminal helix, the 12 Å hole in the center of the pilus measured by x-ray diffraction data would likely be mostly filled with the hydrophobic side chains from this helix. The center of the pilus will have a hydrophobic character and thus could not support the movement of nucleic acids through the central channel of the pilus.

for association of the globular portion of the monomer (Fig. 5*A*). In this model, the negatively charged area on one "side" of the molecule interacts with the positively charged area on the opposite "side." This causes an offset of the monomers and a distinctive curvature to the pilus such that ~5 monomers associate to form one twist of the left-handed helix. In solution, the coulombic forces holding these monomers together would not be strong enough to mediate oligomer formation due to solvation of the charged residues. However, in the pilus these interactions would be complementary possibly resulting in exclusion of water from the electrostatic interface resulting in a stabilization of the pilus as a whole. Since electrostatic interactions are easier to disrupt than hydrophobic interactions, lengthening and shortening of the pilus would be a less energetically costly event.

A previous model, based on the x-ray crystal structure of *N. gonorrhoeae* pilin (15), proposed a symmetric pilus with five subunits per turn and a helical pitch of ~41 Å. While our model agrees that ~5 subunits join to become one turn of the pilus helix, the two models differ in the sense that the model presented here is a left-handed helix (dictated by the electrostatic surfaces) as opposed to a right-handed helix proposed by Parge *et al.* (15, 53). Furthermore, the left-handed helix allows for better packing such that the inner and outer diameters more closely approximate those seen in the x-ray fiber diffraction data.

The x-ray fiber diffraction data suggests there is a 12-Å "hole" in the center of the pilus. Although we observe this with our truncated K122-4 pilin pilus model (Fig. 6*B*), this "hole" is at least partially filled by the hydrophobic side chains of the N-terminal helices in both our model and that of Tainer and co-workers (54). Indeed, it was suggested that this could be the case in the x-ray fiber diffraction data of the pilus (8). Furthermore, due to the fact that the center of the pilus is essentially hydrophobic, passage of DNA or RNA through this center would be energetically unfavorable. However, there may be enough space to allow for small organic molecules to pass. The potential movement of organic molecules through the pilus could allow for intercellular signaling mechanisms.

The fact that DNA or RNA might not be able to pass through the center of the pilus does not necessarily imply that the involvement of type IV pili in DNA transport is minimal. It has been well documented that type IV pili play a role in both episomal gene transfer (55, 56) and DNA transformation (57–59). However, while studies of bacterial conjugation utilizing the F plasmid have clearly indicated the importance of pili in

this process, they have also established that DNA transfer occurs only after a stable mating pair is formed and does not appear to involve the F pilus directly (60–63). It might then be suggested that type IV pilus involvement in DNA transport is minimal as well. If the pilus does play an active role in DNA transport, the model of the K122-4 pilus presented here suggests a different mechanism other than movement through the center of the pilus. Our model reveals a highly positively charged surface that coils around the filament (Fig. 6*C*) where the negatively charged DNA could potentially bind. Upon pilus retraction, DNA could be transported into the cell. Pilus-specific phage could also interact with the pilus, releasing their nucleic acid which could then bind to the surface of the pilus and thus be actively transported into the cell by retraction. These structure-based hypotheses suggest that alteration of the surface charge characteristics of the pilus would alter both DNA transformation and phage sensitivity as well as disrupt the DNA transport and conjugation systems. These are testable hypotheses and are currently under investigation in our laboratory.

The importance of charged residues in forming proper pili is exemplified by the fact that a Glu to Lys mutation at position 5 of the pilin monomer (Fig. 6*E*) disrupts pilus formation (53). The electrostatic repulsion of the lysine to obviously a basic site (possibly $Arg^{30}$) on the surface of one of the globular domains in the pilus results in no pilus formation. In addition, if the mutated pilin is co-expressed with wild-type pilin, it is easy for one to envisage favorable and unfavorable interactions occurring resulting in a pilus that will be kinked.

The structure of K122-4 $pilin^{(29-150)}$ presented here is a paradigm for understanding how pilin monomers associate to form the intact pilus structure. These structures are important in that they allow us a better understanding of the immunological and receptor binding properties of this protein. In addition, the results presented here will aid in the development of anti-adhesive therapeutic strategies and help to design vaccines for *P. aeruginosa*.

*Acknowledgments*—We thank L. Spyracopoulos, C. McInnes, P. Lavigne, and R. Read for valuable discussions. We acknowledge G. McQuaid and S. Gagné for maintenance and operation of NMR spectrometers, respectively, and Prof. L. E. Kay for pulse sequences. We gratefully acknowledge the technical assistance of M. Kaplan, D. Bautista, L. Glasier, W. Wong, C. Grant, and L. Hicks. 800 MHz NMR spectra were acquired at the Canadian National High Field NMR Center (NANUC).

REFERENCES

1. Bodey, G. P., Bolivar, R., Fainstein, V., and Jadeja, L. (1983) *Rev. Infect. Dis.* **5,** 279–313
2. Pier, G. B. (1985) *J. Infect. Dis.* **151,** 575–580
3. Irvin, R. T. (1993) in *Pseudomonas aeruginosa as an Opportunistic Pathogen* (Campa, M., Bendinelli, M., and Friedman, H., eds) pp. 19–42, Plenum Publishing Corp., New York
4. Paranchych, W., Sastry, P. A., Volpel, K., Loh, B. A., and Speert, D. P. (1986) *Clin. Invest. Med.* **9,** 113–118
5. Lee, K. K., Doig, P., Irvin, R. T., Paranchych, W., and Hodges, R. S. (1989) *Mol. Microbiol.* **3,** 1493–1499
6. Bradley, D. E. (1980) *Can. J. Microbiol.* **26,** 146–154
7. Roncero, C., Darzins, A., and Casadaban, M. J. (1990) *J. Bacteriol.* **172,** 1899–1904
8. Folkhard, W. F., Marvin, D. A., Watts, T. H., and Paranchych, W. (1981) *J. Mol. Biol.* **149,** 79–93
9. Merz, A. J., So, M., and Sheetz, M. P. (2000) *Nature* **407,** 98–102
10. Mattick, J. S., Whitchurch, C. B., and Alm, R. A. (1996) *Gene* (*Amst.*) **179,** 147–155
11. Lee, K. K., Sheth, H. B., Wong, W. Y., Sherburne, R., Paranchych, W., Hodges, R. S., Lingwood, C. A., Krivan, H., and Irvin, R. T. (1994) *Mol. Microbiol.* **11,** 705–713
12. Rini, J. M. (1995) *Annu. Rev. Biophys. Biomol. Struct.* **24,** 551–577
13. Campbell, A. P., McInnes, C., Hodges, R. S., and Sykes, B. D. (1995) *Biochemistry* **34,** 16255–16268
14. Campbell, A. P., Sheth, H. B., Hodges, R. S., and Sykes, B. D. (1996) *Int. J. Pept. Protein Res.* **48,** 539–552
15. Parge, H. E., Forest, K. T., Hickey, M. J., Christensen, D. A., Getzoff, E. D., and Tainer, J. A. (1995) *Nature* **378,** 32–38
16. Hazes, B., Sastry, P. A., Hayakawa, K., Read, R. J., and Irvin, R. T. (2000) *J. Mol. Biol.* **299,** 1005–1017
17. Ramphal, R., Sadoff, J. C., Pyle, M., and Silipigni, J. D. (1984) *Infect. Immun.* **44,** 38–40
18. Ramphal, R., Carnoy, C., Fievre, S., Michalski, J. C., Houdret, N., Lamblin, G., Strecker, G., and Roussel, P. (1991) *Infect. Immun.* **59,** 700–704
19. Sheth, H. B., Lee, K. K., Paranchych, W., Hodges, R. S., and Irvin, R. T. (1994) *Mol. Microbiol.* **11,** 715–723
20. Yu, L., Lee, K. K., Hodges, R. S., Paranchych, W., and Irvin, R. T. (1994) *Infect. Immun.* **62,** 5213–5219
21. Alonso, A., Companario, E., and Martinez, J. L. (1999) *Microbiology* **145,** 2857–2862
22. Cryz, S. J., Fürer, E., and Germanier, R. (1983) *Infect. Immun.* **39,** 1072–1079
23. Lydick, E., McClean, A. A., Woodhour, A. F., and Callahan, L. T. (1985) *J. Infect. Dis.* **151,** 375
24. Finke, M., Muth, G., Reichhelm, T., Thoma, M., Duchene, M., Hungerer, K. D., Domdey, H., and von Specht, B. U. (1991) *Infect. Immun.* **59,** 1251–1254
25. Pier, G. B., and Thomas, D. M. (1983) *J. Infect. Dis.* **148,** 206–213
26. Pugh, G. W., Hughes, D. E., and Booth, G. D. (1977) *Am. J. Vet. Res.* **38,** 1519–1522
27. Farinha, M. A., Conway, B. D., Glasier, L. M. G., Ellert, N. W., Irvin, R. T., Sherburne, R., and Paranchych, W. (1994) *Infect. Immun.* **62,** 4118–4123
28. Sheth, H. B., Glasier, L. M., Ellert, N. W., Cachia, P., Kohn, W., Lee, K. K., Paranchych, W., Hodges, R. S., and Irvin, R. T. (1995) *Biomedical Peptides Proteins Nucleic Acids* **1,** 141–148
29. Cachia, P. J., Glasier L. M., Hodgins, R. R., Wong, W. Y., Irvin, R. T., and Hodges, R. S. (1998) *J. Peptide Res.* **52,** 289–299
30. Tripet, B., Yu, L., Bautista, D. L., Wong, W. Y., Irvin, R. T., and Hodges, R. S. (1996) *Protein Eng.* **9,** 1029–1042
31. Johnson, M. L., Correia, J. J., Yphantis, D. A., and Halvorson, H. R. (1981) *Biophys. J.* **36,** 575–588
32. Delaglio, F., Grzesiek, S., Vuister, G. W., Zhu, G., Pfeifer, J., and Bax, A. (1995) *J. Biomol. NMR* **6,** 277–293
33. Johnson, B. A., and Blevins, R. A. (1994) *J. Biomol. NMR* **4,** 603–614
34. Keizer, D. W., Kalisiak, M., Crump, M. P., Suh, J. Y., Irvin, R., and Sykes, B. D. (2001) *J. Biomol. NMR,* **19,** 385–386
35. Nilges, M., and O'Donoghu, S. I. (1998) *Prog. Nuclear Mag. Res. Spectrosc.* **32,** 107–139
36. Brünger, A. T. (1993) in *X-PLOR Version 3.1*: *A System for X-ray Crystallography and NMR*, Yale University Press, New Haven, CT
37. Vuister, G. W., and Bax, A. (1993) *J. Am. Chem. Soc.* **115,** 7772–7777
38. Gagné, S. M., Tsuda, S., Li, M. X., Chandra, M., Smillie, L. B., and Sykes, B. D. (1994) *Protein Sci.* **3,** 1961–1974
39. Paranchych, W., Sastry, P. A., Frost, L. S., Carpenter, M., Armstrong, G. D., and Watts, T. H. (1979) *Can. J. Microbiol.* **25,** 1175–1181
40. Pennington, J. E., and Williams, R. M. (1979) *J. Infect. Dis.* **139,** 396–400
41. Suh, J. Y., Spyracopoulos, L., Keizer, D. W., Irvin, R. T., and Sykes, B. D. (2001) *Biochemistry,* **40,** 3985–3995
42. Campbell, A. P., Wong, W. Y., Houston, M., Schweizer, F., Cachia, P. J., Irvin, R. T., Hindsgaul, O., Hodges, R. S., and Sykes, B. D. (1997) *J. Mol. Biol.* **267,** 382–402
43. Haas, R., Schwarz, H., and Meyer, T. F. (1987) *Proc. Natl. Acad. Sci. U. S. A.* **84,** 9079–9083
44. Marrs, C. F., Ruehl, W. H., Schoolnik, G. K., and Falkow, S. (1988) *J. Bacteriol.* **170,** 3032–3039
45. Long, C. D., Madraswala, R. N., and Seifert, H. S. (1998) *Infect. Immun.* **66,** 1918–1927
46. Swanson, J., Robbins, K., Barrera, O., and Koomey, J. M. (1987) *J. Exp. Med.* **165,** 1016–1025
47. Marrs, C. F., Rozsa, F. W., Hackel, M., Stevens, S. P., and Glasgow, A. C. (1990) *J. Bacteriol.* **172,** 4370–4377
48. Meyer, T. F., Gibbs, C. P., and Haas, R. (1990) *Annu. Rev. Microbiol.* **44,** 451–477
49. McInnes, C., Sönnichsen, F. D., Kay, C. M., Hodges, R. S., and Sykes, B. D. (1993) *Biochemistry* **32,** 13432–13440
50. Watts, T. H., Scraba, D. G., and Paranchych, W. (1982) *J. Bacteriol.* **151,** 1508–1513
51. Birnboim, H. C., and Doly, J. (1979) *Nucleic Acids Res.* **7,** 1513–1523
52. Beard, M. K. M., Mattick, J. S., Moore, L. J., Mott, M. R., Marrs, C. F., and Egerton, J. R. (1990) *J. Bacteriol.* **172,** 2601–2607
53. Pasloske, B. L., Scraba, D. G., and Paranchych, W. (1989) *J. Bacteriol.* **171,** 2142–2147
54. Forest, K, T., and Tainer, J. A. (1997) *Gene* (*Amst.*) **192,** 165–169
55. Kim, S.-R, and Komano, T. (1997) *J. Bacteriol.* **179,** 3594–3603
56. Karaolis, D. K., Somara, S., Maneval, D. R., Johnson, J. A., and Kaper, J. B. (1999) *Nature* **399,** 375–379
57. Fussenegger, M., Rudel, T. Barten, R., Ryll, R., and Meyer, T. F. (1997) *Gene* (*Amst.*) **192,** 125–134
58. Wolfgang, M., Lauer, P., Park, H. S., Brossay, L., Hebert, J., and Koomey, M. (1998) *Mol. Microbiol.* **29,** 321–330
59. Wolfgang, M., van Putten, J. P., Hayes, S. F., and Koomey, M. (1999) *Mol. Microbiol.* **31,** 1345–1357
60. Durrenberger, M. B., Villiger, W., and Bachi, T. (1991) *J. Struct. Biol.* **107,** 146–156
61. Haase, J., Lurz, R., Grahn, A. M., Bamford, D. H., and Lanka, E. (1995) *J. Bacteriol.* **177,** 4779–4791
62. Klimke, W. A., and Frost, L. S. (1998) *J. Bacteriol.* **180,** 4036–4043
63. Silverman, P. M. (1997) *Mol. Microbiol.* **23,** 423–429
64. Wishart, D. S., Boyko, R. F., and Sykes, B. D. (1994) *Comput. Appl. Biosci.* **10,** 687–688